Live imaging of chronic inflammation caused by mutation of zebrafish Hai1

Jonathan R. Mathias[1], M. Ernest Dodd[1], Kevin B. Walters[1], Jennifer Rhodes[2], John P. Kanki[2], A. Thomas Look[2] and Anna Huttenlocher[1,*]

[1]Department of Medical Microbiology and Immunology, University of Wisconsin-Madison, Madison, WI 53706, USA
[2]Department of Pediatric Oncology, Dana-Farber Cancer Institute, Boston, MA 02115, USA
*Author for correspondence (e-mail: huttenlocher@wisc.edu)

Accepted 17 August 2007
Journal of Cell Science 120, 3372-3383 Published by The Company of Biologists 2007
doi:10.1242/jcs.009159

Summary

The hallmark of chronic inflammation is the infiltration and persistence of leukocytes within inflamed tissue. Here, we describe the first zebrafish chronic inflammation mutant identified in an insertional mutagenesis screen for mutants that exhibit abnormal tissue distribution of neutrophils. We identified a mutant line with an insertion in the Hepatocyte growth factor activator inhibitor 1 gene (*hai1*; also known as *Spint1*) that showed accumulation of neutrophils in the fin. The mutant embryos exhibited inflammation in areas of epidermal hyperproliferation that was rescued by knock-down of the type II transmembrane serine protease Matriptase 1 (also known as St14), suggesting a novel role for Hai1-Matriptase 1 pathway in regulating inflammation. Using time-lapse microscopy of mutant embryos that express GFP from a neutrophil-specific promoter, we found that individual neutrophils in inflamed tissue displayed random motility characterized by periods of pausing alternating with periods of motility. During periods of persistent movement the cells were highly polarized, while the pausing modes were characterized by a loss of cell polarity. In contrast to responses to acute injury, neutrophils did not exhibit clear retrograde chemotaxis or resolution of inflammation in the mutant. These findings illustrate the utility of zebrafish as a new model system to study chronic inflammation and to visualize immune responses with high resolution in vivo.

Supplementary material available online at
http://jcs.biologists.org/cgi/content/full/120/19/3372/DC1

Key words: Cell migration, Inflammation, Neutrophil, Psoriasis, Zebrafish

Introduction

The hallmark of chronic inflammation is the infiltration and persistence of leukocytes within inflamed tissue. Neutrophils are the first responders to inflammatory stimuli such as bacterial infection or tissue injury and are required for normal host responses to infection. However, the inappropriate recruitment and retention of neutrophils within tissues is central to the pathogenesis of chronic inflammatory disease. Chemotaxis is the fundamental process underlying neutrophil recruitment, however, in the case of many chronic inflammatory diseases this recruitment appears to occur in the absence of inciting stimuli such as infection. Despite progress in understanding neutrophil function and chemotaxis in vitro, the mechanisms of neutrophil recruitment and retention in the context of chronic inflammation in vivo remain largely unknown. Therefore, the development of improved experimental systems for studying neutrophil chemotaxis and recruitment in vivo is a critical goal for increasing our understanding of the pathogenesis of chronic inflammatory disease.

The zebrafish, *Danio rerio*, has emerged as a powerful model system to examine mechanisms of human disease because it is a vertebrate that is genetically tractable and is amenable to small molecule screening (Patton and Zon, 2001; Zon and Peterson, 2005). The presence of both innate and adaptive immune systems in zebrafish provides support for the utility of zebrafish as a tool to examine the role of immune cells in normal development and in the pathogenesis of disease states (Crowhurst et al., 2002; de Jong and Zon, 2005; Langenau and Zon, 2005; Murayama et al., 2006; Onnebo et al., 2004; Trede et al., 2004). For example, substantial evidence indicates the validity and strength of using zebrafish to examine host-pathogen interactions in vivo in response to mycobacterial (Davis et al., 2002) or other (van der Sar et al., 2003) infections that can be observed in real-time because of the optical clarify of zebrafish embryos. Further clarification of these immune responses can be provided by recent advances in the generation of transgenic zebrafish in which specific cell lineages, including lymphocytes (Langenau et al., 2004), macrophages (Hall et al., 2007) and neutrophils (Mathias et al., 2006; Meijer et al., 2007; Renshaw et al., 2006) are marked with fluorescent proteins such as green fluorescent protein (GFP). These transgenic zebrafish can be used to provide high-resolution analysis of leukocyte development and trafficking (Mathias et al., 2006; Redd et al., 2006), and provide significant insight into the evolution of the inflammatory response. Despite progress in characterizing the zebrafish immune system, no zebrafish models of human chronic inflammatory diseases have been developed to date.

To identify zebrafish models of chronic inflammation, we screened a collection of mutant zebrafish embryos for those that display abnormal tissue distributions of neutrophils. A

Journal of Cell Science

Journal of Cell Science

recent large-scale insertional mutagenesis project (Amsterdam et al., 1999) produced a collection of mutant zebrafish whose mutations can be mapped relatively quickly when compared to traditional approaches. Several of these mutants have been mapped and display morphological phenotypes that can be viewed within 5 days post-fertilization (dpf) (Amsterdam et al., 2004). In this study we show that one of these mutants, bearing an insertion within the hepatocyte growth factor activator inhibitor 1 (*hai1*; also known as *spint1*) gene, exhibits a phenotype similar to chronic inflammation consisting of neutrophil and macrophage infiltration into the fin of the fish.

In mammals HAI1 has been shown to be a cell surface-bound serine protease inhibitor that has been shown to limit the activity of hepatocyte growth factor activator (HGFA) (Shimomura et al., 1997) and matriptase (Benaud et al., 2001), and is required for mouse development (Fan et al., 2006; Tanaka et al., 2005). Hepatocyte growth factor (HGF) is a mitogen for several cell types, and is activated (potentially by HGFA and other proteases) at sites of tissue injury (Miyazawa et al., 1994). Matriptase 1 (also known as ST14) is a type II transmembrane serine protease originally isolated from breast cancer cells and shown to degrade extracellular matrix proteins (Shi et al., 1993). Matriptase can also proteolytically activate HGF and urokinase-type plasminogen activator (Lee et al., 2000). Overexpression of matriptase in mouse skin cells causes spontaneous squamous cell carcinoma and other phenotypes consistent with malignant epithelial transformation, including dermal inflammation (List et al., 2005).

Here we show that *hai1* mutant zebrafish embryos exhibit inflammation in areas of epidermal hyperproliferation, a phenotype that resembles the common human skin disease psoriasis. Using time-lapse fluorescent microscopy of optically transparent mutant embryos that express GFP in neutrophils, we tracked the migration of individual neutrophils within the inflamed epithelium. We found that neutrophils in the inflamed fin display a biased random migration with frequent pauses. The mutant phenotype can be rescued by knock-down of Matriptase 1, suggesting that Matriptase 1 is a key effector downstream of Hai1 that regulates epidermal proliferation and inflammation. This study illustrates the utility of zebrafish as a new model system to study chronic inflammation and to visualize immune responses with high resolution in real-time.

Results

Identification of *hi2217* mutant inflammation phenotype

To identify genes that are involved in regulating inflammation, a collection of zebrafish insertional mutants (Amsterdam et al., 1999) was screened for expression of the neutrophil-specific zebrafish myeloperoxidase (MPO; also known as Mpx) gene (Bennett et al., 2001; Lieschke et al., 2001). Embryos were screened by in situ hybridization of *MPO* mRNA at 2 dpf to identify mutants with an inflammation phenotype. We identified three lines from 276 lines screened that displayed abnormal tissue distribution of neutrophils. One of these was the *hi2217* mutant line, which bears an insertion within the promoter of the zebrafish *hai1* gene (Fig. 1A) and has been partially characterized in a screen for genes required

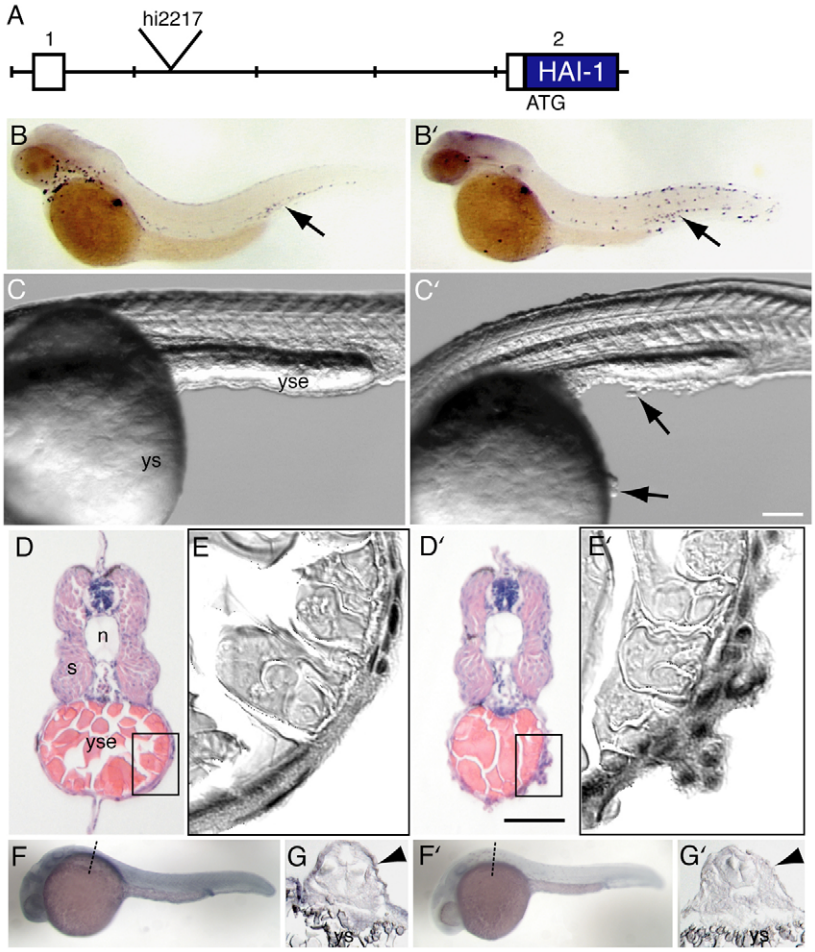

Fig. 1. The *hi2217* mutant exhibits a chronic inflammation phenotype and reduced expression of Hai1. (A) Genomic map of *hi2217* insertion; exons are depicted as numbered boxes, and the start of the Hai1 (HAI-1) open reading frame (blue) is indicated (ATG); each section equals 500 bp. (B-F′) Images of *hi2217* embryos; B-G are wild-type siblings, B′-G′ are mutants. (B,B′) In situ hybridization of zebrafish MPO at 2 dpf, arrows indicate the position of the intermediate cell mass (ICM), the location of neutrophil development in zebrafish embryos. (C,C′) Oblique coherent contrast (OCC) images of live *hi2217* embryos at 26 hpf, arrows indicate clusters of rounded cells on the yolk sac (ys) and yolk sac extension (yse) of the mutant. (D-E′) Hematoxylin and Eosin-stained transverse sections of *hi2217* embryos at 2 dpf, at the level of the yolk sac extension (yse); s, somites; n, notochord. D,D′ are full views; E,E′ are magnified views of the boxed areas in D,D′. (F-G′) In situ hybridization of Hai1 at 30 hpf. (F,F′) Whole-mount and (G,G′) frozen sections at the level of the yolk sac, which is indicated by dashed lines in F,F′; arrowheads indicate the epidermis. Whole embryos are oriented anterior to the left, dorsal side up; sections oriented dorsal side up. Bars, 200 μm.

Journal of Cell Science

for embryonic development (Amsterdam et al., 2004). Mutant embryos homozygous for the *hi2217* insertion demonstrated an abnormal distribution of MPO-expressing cells as compared to wild-type siblings, with infiltration of neutrophils into the zebrafish fin (Fig. 1B,B′). Homozygous mutant fish can be identified as early as 26 hours post-fertilization (hpf) by the formation of rounded cells over the yolk sac and degradation of the anterior end of the yolk sac extension (Fig. 1C,C′), and by 2 dpf display a rough tailfin phenotype and disruption of the normal fin morphology (discussed later). Transverse sections of embryos at 2 dpf indicated that the epidermis of mutant embryos is disorganized and thickened, with groups of overlapping, rounded epidermal cells (Fig. 1D′,E′) in contrast to the ordered two-cell epithelial layer found in wild-type embryos (Fig. 1D,E). In situ hybridization has shown that *hai1* is expressed in the epidermis of developing zebrafish embryos (Thisse et al., 2001). We observed a similar pattern of *hai1* expression in wild-type siblings (Fig. 1F,G) that is reduced in homozygous mutant *hi2217* embryos (Fig. 1F′,G′). Together, these findings indicate that we have identified a zebrafish mutant with infiltration of neutrophils into the zebrafish fin and hallmarks of chronic inflammation associated with disruption of the epidermis. Furthermore, our findings suggest a novel function for zebrafish Hai1 as a tissue-specific regulator of the inflammatory response.

Inflammation is an early component of the *hi2217* mutant phenotype

To determine the developmental progression of inflammation in the mutant embryos, we characterized the phenotype at different developmental stages. At 26 hpf at the onset of the epithelial phenotype, we did not observe neutrophil mislocalization by either immunofluorescence or in situ hybridization (data not shown), probably due to the fact that few neutrophils are present at 26 hpf (Lieschke et al., 2001). By contrast, when we used a macrophage-specific L-plastin antibody (Fig. S1A-C in supplementary material) we found that macrophages are recruited to the areas of rounded cells in mutant embryos at 26 hpf (supplementary material Fig. S1D′). These findings suggest that inflammation is an early component of the phenotype in the *hai1* mutant fish.

To determine the onset of neutrophilic inflammation within the tailfin, we used a neutrophil-specific antibody that labels MPO (Mathias et al., 2006). Zebrafish neutrophils can be detected in the fins of mutant but not control embryos as early as 36 hpf (Fig. 2B,B′) and accumulate in areas with rounding of tailfin cells (Fig. 2A,A′). By 48 hpf the tailfins of *hi2217* mutant embryos are thinner, appear degraded (Fig. 3A′) and are fully infiltrated by neutrophils (Fig. 3B′) and macrophages (Fig. 3C′). The infiltration of neutrophils and macrophages into the tailfin persists at 5 dpf (data not shown). The areas of the fin that exhibit neutrophilic infiltration do not appear to have enhanced apoptosis (Fig. 2C,C′). Prevention of apoptosis by injection of a morpholino oligonucleotide (MO) to p53 (Langheinrich et al., 2002) or treatment with a caspase inhibitor (Renshaw et al., 2006) had no significant effect on the neutrophilic inflammation in the zebrafish fin at 2 dpf (data not shown). Together these findings suggest that the neutrophilic inflammation into the tailfins of *hi2217* mutants is not induced by apoptosis.

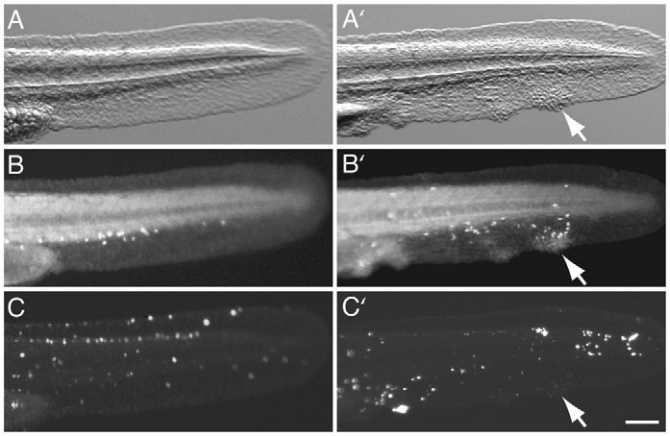

Fig. 2. Onset of neutrophilic inflammation in *hi2217* mutants at 36 hpf. Tailfin views of *hi2217* embryos fixed at 36 hpf; A-C are wild-type siblings, A′-C′ are mutants. (A,A′) OCC images and corresponding images of zMPO immunolabeling (B,B′) and TUNEL (C,C′) from the same embryo; arrows indicate the same group of rounded cells in A′-C′. Embryos are oriented anterior to the left, dorsal side up. Bars, 100 μm.

Mutant embryos exhibit enhanced epidermal proliferation and disruption of the epithelial morphology

To further characterize the epithelial phenotype in the mutant embryos we characterized cell proliferation and integrity of epithelial cell-cell contacts in mutant and control embryos. Since areas in the fin that displayed cell rounding and a less differentiated phenotype were not associated with apoptosis, we determined whether cell proliferation was different in mutant and control embryos. The mutant fins exhibited enhanced cell proliferation (detected by BrdU labeling; Fig. 3D′, Fig. 4C′), suggesting that the mutant phenotype is associated with hyperproliferation of tailfin cells, which are primarily epithelial in nature. These findings are in accordance with a recent publication that indicates that disruption of Hai1-regulated processes induces epidermal proliferation (List et al., 2005). Cell borders were labeled using a pan-cadherin antibody, which showed that the normal epithelial organization of tailfin cells (Fig. 3E) was disorganized with overlapping cells in mutant embryos (Fig. 3E′). Together these findings suggest that mutant embryos display epithelial hyperproliferation coupled with inflammation, a phenotype that resembles the common skin condition psoriasis.

Inflammation is not required for the early epithelial phenotype

To determine if leukocytes cause the mutant phenotype, we depleted the embryos of macrophages and neutrophils by injection of a MO targeting pu.1 (also known as Spi1), a transcription factor required for the development of both of these cell types (Rhodes et al., 2005). The pu.1 MO blocked the development of macrophages (supplementary material Fig. S1G,G′) without preventing the cell rounding and degradation of the yolk sac extension seen in mutants at 26 hpf (supplementary material Fig. S1G′). Injection of the pu.1 MO also blocked the development of neutrophils (Fig. 4E,E′) without preventing the epidermal phenotype and enhanced proliferation observed in mutant tailfins at 38 hpf (Fig. 4D′,F′)

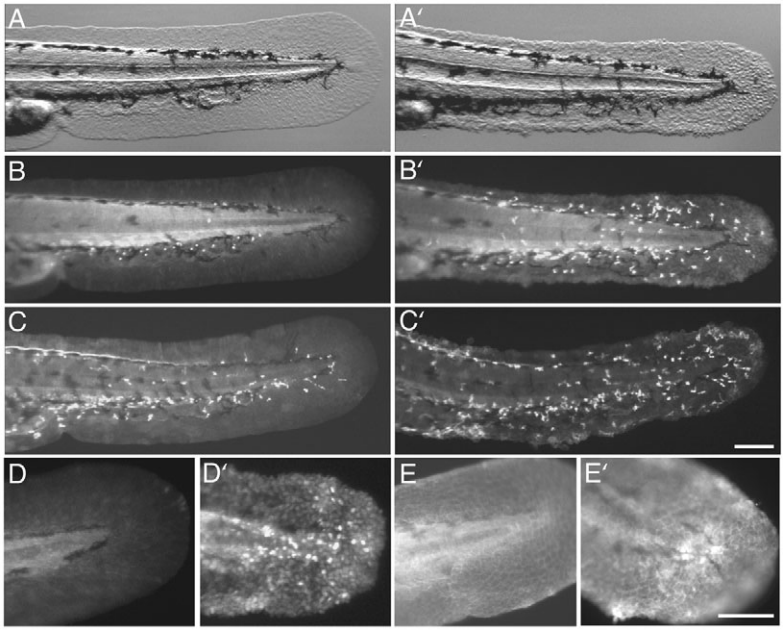

Fig. 3. *hi2217* mutant phenotypes at 48 hpf. Tailfin views of *hi2217* embryos fixed at 48 hpf; A-E are wild-type siblings, A′-E′ are mutants. (A,A′) OCC images and corresponding images of zMPO immunolabeling (B,B′) of the same embryo; (C,C′) L-Plastin immunolabeling in different embryos; (D,D′) BrdU immunolabeling; (E,E′) Pan-Cadherin immunolabeling. Embryos are oriented anterior to the left, dorsal side up. Bars, 100 μm.

indicating that these early phenotypes are not the result of neutrophil-mediated inflammation. However, we were unable to determine if neutrophils or macrophages were involved in the progression of the fin phenotype at later stages, because the pu.1 MO was not effective at completely knocking out zebrafish neutrophils and macrophages in mutants past 2 dpf (data not shown). Taken together, these findings suggest that the induction of the epithelial phenotypes observed in the *hai1* mutants is independent of the inflammatory changes.

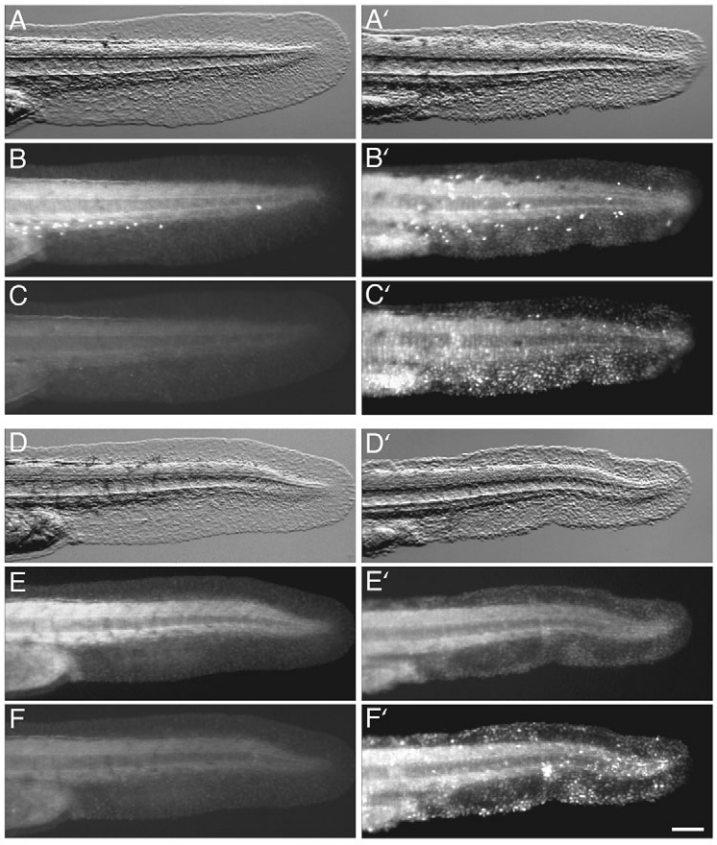

Fig. 4. *hi2217* mutant epithelial phenotypes at 38 hpf are not mediated by leukocytes. Tailfin views of *hi2217* embryos pulse-labeled with BrdU and fixed at 38 hpf; A-F are wild-type siblings, A′-F′ are mutants. (A,A′,D,D′) OCC images and corresponding images of zMPO immunolabeling (B,B′,E,E′) and BrdU immunolabeling (C,C′,F,F′) of uninjected (A-C,A′-C′) and *pu.1* MO-injected (D-F,D′-F′) *hi2217* embryos. Embryos are oriented anterior to the left, dorsal side up. Bar, 100 μm.

MO-mediated knock-down of *hai1* reproduces the *hi2217* mutant phenotype

To confirm that Hai1 mediates the inflammation and epithelial phenotypes observed in mutant embryos, we used a MO to zebrafish *hai1* to deplete embryos of Hai1. Injection of the *hai1* MO into wild-type embryos was observed to recapitulate the phenotypes observed in the *hi2217* mutants (Fig. 5A′-C′), whereas injection of either a standard control MO or 5-base mismatch MO had no effect (Fig. 5A-C). In *hai1* morphants at 24 hpf rounded cells over the yolk sac extension were observed (Fig. 5A′), as well as tailfin degradation (Fig. 5B′), and by 48 hpf, the infiltration of neutrophils (Fig. 5C′) and macrophages (data not shown) into tailfins. To determine the effect of knocking down *hai1* expression in a subset of embryonic cells, we injected the *hai1* MO into single cells at the 8- to 16-cell stage of embryonic development to asymmetrically distribute the MO. At 2 dpf these embryos often exhibited localized manifestations of rounded cell clusters in an otherwise morphologically wild-type embryo (Fig. 5D), whereas embryos similarly injected with the 5-base mismatch *hai1* MO retained the wild-type morphology (data not shown). Neutrophils were recruited to these localized regions of cell rounding (Fig. 5E) in *hai1* morphants, suggesting that changes in the localized environment, induced by reduction of Hai1, induce both the epithelial phenotype and leukocyte recruitment. These data, in conjunction with the *hai1* in situ hybridization data (Fig. 1F-G′), indicate that loss of Hai1 results in the observed *hi2217* mutant phenotypes.

Matriptase 1 is required for the inflammation and epidermal phenotype in the *hi2217* mutant

Previous studies have demonstrated that the type II transmembrane serine protease Matriptase 1 has strong oncogenic effects (Oberst et al., 2001; Santin et al., 2003) and is negatively regulated by Hai1 (Benaud et al., 2001). Overexpression of matriptase in mouse skin cells (List et al., 2005) resulted in many of the phenotypes that we observe in the *hi2217* mutant zebrafish, including

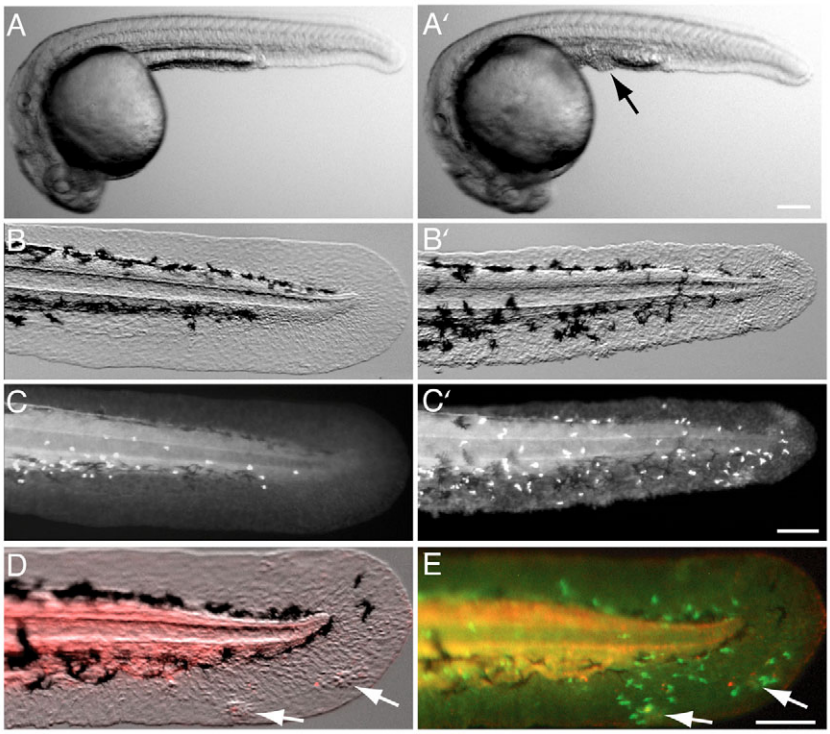

Fig. 5. Injection of *hai1* MO into wild-type embryos phenocopies the *hi2217* mutant. Shown are images of wild-type embryos at 24 hpf (A,A′) and 48 hpf (B-E) following injection of a standard control MO (A), *hai1* 5-base mismatch MO (B,C) or *hai1* MO (A′-C′). (A,A′) Live OCC images; (B,B′) OCC images and (C,C′) corresponding zMPO immunolabeling in fixed embryos. (D,E) Partial knock-down by co-injection of *hai1* MO and TMR-dextran (to trace injected cells) into 8- to 16-cell wild-type embryos. (D) OCC overlaid with red fluorescence from TMR-dextran, indicating cells that contain the MO, (E) Red fluorescence (TMR-dextran) overlaid onto green zMPO immunolabel. Note the otherwise wild-type morphology of the tailfin (compare to B,B′) with localized areas of rounded cells (arrows) that overlap with red fluorescent cells, to which neutrophils (green) are recruited. Embryos are oriented anterior to the left, dorsal side up. Bars, 100 μm.

inflammatory cell infiltration and epithelial proliferation. In addition, overexpression of HAI1 in this mouse model was shown to abrogate the phenotypes caused by matriptase overexpression. This indicates that the balance between these two proteins may regulate processes that, when disrupted, result in chronic inflammation. Database searches revealed a single predicted open reading frame (accession no. XM_678577) for a zebrafish *matriptase 1* homologue. In situ hybridization (using an overlapping partial cDNA as a probe) showed that zebrafish *matriptase 1* is expressed throughout the epidermis of zebrafish embryos (Fig. 6A), similar to the distribution observed for Hai1 (Fig. 1F). In accordance with the data described above, transient MO-mediated knock-down of zebrafish *matriptase 1* (using either of two non-overlapping MO sequences) rescued the *hi2217* mutant phenotypes, whereas injection of either a 5-base mismatch MO or standard control MO did not (Fig. 6). Embryos injected with *matriptase 1* MO exhibited very few instances of rounded cells over the yolk sac by 30 hpf (Fig. 6B-D,H) and often exhibited bent tails (Fig. 6B). At 48 hpf, *matriptase 1* MO-injected *hi2217* embryo tailfins were not degraded (Fig. 6F,H) and did not exhibit infiltration of neutrophils (Fig. 6I) compared to control MO-injected mutants (Fig. 6G,H,J).

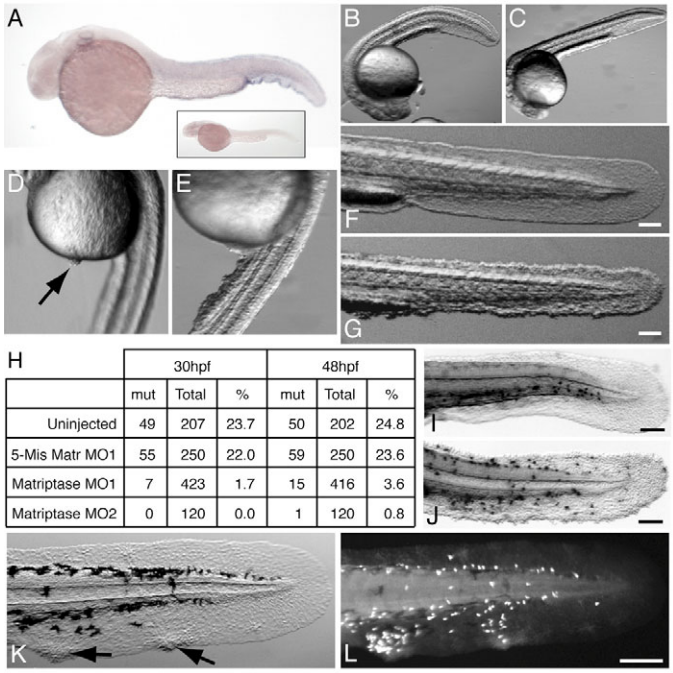

H

	30hpf			48hpf		
	mut	Total	%	mut	Total	%
Uninjected	49	207	23.7	50	202	24.8
5-Mis Matr MO1	55	250	22.0	59	250	23.6
Matriptase MO1	7	423	1.7	15	416	3.6
Matriptase MO2	0	120	0.0	1	120	0.8

Fig. 6. MO-mediated knock-down of *matriptase 1* rescues *hi2217* mutant. (A) In situ hybridization of zebrafish *matriptase 1* in wild-type embryo at 30 hpf; inset shows an embryo labeled with a sense probe from the same plasmid template. (B-G) Live images of *hi2217* embryos injected with either *matriptase 1* MO1 (B,C,D,F) a standard control MO (E) or a 5-base mismatch *matriptase 1* MO1 (G) at 30 hpf (B-E) or 48 hpf (F,G). (H) Quantification of morphological data at 30 and 48 hpf; the number of embryos exhibiting a mutant (mut) morphology (as in D,E,G) were counted for each condition and divided by the total number of embryos to give the percentage that exhibit the mutant phenotype (%). Note that any instance of rounded cells (e.g. that seen in D, even with an otherwise wild-type morphology) was counted as a mutant phenotype. (I,J) MPO activity assay of embryos fixed at 48 hpf following injection with *matriptase 1* MO1 (I) or 5-base mismatch *matriptase 1* MO1 (J). (K,L) Partial phenocopy by injection of a lesser volume of *matriptase 1* MO. OCC (K) and corresponding MPO immunolabeling (L) of an *hi2217* embryo injected with *matriptase 1* MO2 at a concentration less than required for rescue (see Materials and Methods), note the recruitment of neutrophils to localized areas of rounded cells (arrows in K). Note that the similar injection of 5-base mismatch *matriptase 1* MO1 into other embryos resulted in 25% showing a ‘full’ mutant phenotype similar to that seen in G and J (data not shown). Embryos are oriented anterior to the left, dorsal side up (A-C,F-L) or anterior up, dorsal side to the right (D,E). Bars, 100 μm.

Journal of Cell Science

Injection of a smaller volume of *matriptase 1* MO into *hi2217* embryos often yielded 25% of embryos with isolated groups of rounded cells in otherwise wild-type tailfins (Fig. 6K), to which neutrophils were recruited (Fig. 6L); this phenotype is similar to the partial knock-down of *hai1* in wild-type embryos (Fig. 5D,E) and indicates that neutrophils are responding to epithelial disruptions in mutant embryos. Taken together, these findings suggest that the *hi2217* mutant phenotypes are caused by an increase in Matriptase activity due to the reduced expression of its endogenous inhibitor Hai1.

Time-lapse imaging of neutrophil inflammation in vivo

To generate a model in which neutrophil motility could be observed in a chronic inflammatory state, the *hi2217* line was crossed to a transgenic line (*MPO:GFP*) in which neutrophils express GFP (Mathias et al., 2006). Time-lapse microscopy of *hi2217;MPO:GFP* mutant embryos at 2 dpf showed extensive infiltration of highly motile neutrophils into mutant tailfins (see Movie 1 in supplementary material). Individual neutrophils were tracked (Fig. 7A) and basic parameters of cell migration were analyzed for long durations (average 82 minutes). The average cell speed was 6.5±2.2 μm/minute and the cells exhibited low directional persistence over extended durations, with a D/T ratio of 0.27 (D/T>0.7 considered directed migration). Individual neutrophil migration was characterized by periods of motility alternating with frequent pauses (Fig. 7B,C), similar to what is observed in migrating primordial germ cells, which exhibit frequent pauses or 'tumbling' modes alternating with periods of rapid migration or 'running' (Reichman-Fried et al., 2004). These behavioral modes in *hi2217* neutrophils appeared to be independent of the cellular environment since individual neutrophils did not share common tracks and cells generally did not simultaneously accumulate in specific areas. During active migration *hi2217* neutrophils take on a highly polarized morphology and were often very protrusive (Fig. 7B-D, Movie 2 in supplementary material), whereas pauses were characterized by a loss of polarity, cell rounding and extension of pseudopodia in multiple directions (Fig. 7B-D). Mutant neutrophils were observed to pause frequently (moving <0.75 μm/minute, for an average of 16% of the time; see Fig. 7E), and cells that paused more frequently were found to have lower average velocities (Fig. 7E). When analyzed over 15-minute windows, periods of directional migration with intervening periods of random movement were often apparent (Fig. 7F-I). Whereas some tracks showed correlation between changes in velocity and directional persistence (Fig. 7F,G), others showed that there was no significant correlation between these parameters (Fig. 7H,I). Some migratory GFP-positive cells in the mutants were observed to undergo mitosis, with continued migration after cell division (Movie 1 in supplementary material). Since neutrophils are terminally differentiated cells, this probably indicates that neutrophil precursors [which express zMPO (Hsu et al., 2004; Lieschke et al., 2001)] are contributing to the inflammatory response in mutants, which emphasizes the severity of the mutant phenotype. In summary, zebrafish neutrophils exhibit highly dynamic motility in the context of chronic inflammation in vivo, characterized by periods of rapid movement alternating with stopping or pausing.

Recent studies have indicated highly directed migration of zebrafish neutrophils in vivo in response to acute injury (Mathias et al., 2006). To compare the migration of zebrafish neutrophils in response to acute and chronic inflammatory stimuli, the migration parameters in mutant embryos were compared to the migration induced in response to acute tissue injury in sibling control embryos at 2 dpf. Since tracks in unwounded mutants were considerably longer (average 82 minutes) than in the wild type (average 12 minutes), parameters were calculated for the mutant embryos during the first 12 minutes of each track. The average cell velocity for neutrophils in mutant embryos (6.3±3.2 μm/minute) was less than the migration of cells to the wound in wild-type siblings (8.1±2.3 μm/minute; Fig. 8A,B). Calculation of directional persistence values indicated that mutant neutrophils moved in a less directional manner compared to wild-type counterparts in response to a wound (Fig. 8A,B). Further analysis of average mean displacements (Sumen et al., 2004) indicated that the mutant neutrophils generally moved in a random walk fashion as compared to the directed migration of neutrophils to a wound in wild type embryos (Fig. 8C). However, analysis of individual mutant cell tracks indicates that the cells can in fact move directionally over short periods of time (Fig. 7F-I). Whereas neutrophils from wild-type embryos exhibit retrograde chemotaxis to the vasculature at 2 dpf (data not shown) and 3 dpf (Mathias et al., 2006), we did not see clear evidence of directed movement toward the vasculature or resolution of inflammation in the mutant embryos.

To determine whether mutation of *hai1* caused a cell autonomous defect in neutrophils that resulted in the slower, less directed motility observed in the mutants, we characterized the neutrophil response to acute tissue injury in mutant embryos. Wounding of mutant embryo tailfins induced a robust and localized inflammatory response (Fig. 8D,E), similar to that observed in wild-type embryos. Neutrophils were tracked to wounds in mutant embryos, and in contrast to wild-type embryos, the majority of the neutrophils (67%) were recruited from the tailfin rather than from the vasculature. Calculation of migration parameters indicated that mutant neutrophils moved directionally in response to tissue injury (Fig. 8A,B) at a speed that is generally faster than wild-type neutrophils, suggesting that the chronic inflammatory environment may prime neutrophils to have a more robust response to acute injury. Together the findings indicate that the chronic inflammation observed in mutant embryos is not likely mediated by a primary defect in neutrophil function since mutant neutrophils retain the ability to display highly directed migration in response to acute injury even in the context of a chronic inflammatory environment.

Effect of NS-398 on neutrophil motility in vivo

To determine the utility of the *hi2217;MPO:GFP* model to test the effects of specific drug treatments on motility and inflammatory responses in vivo, we tested the effects of a non-steroidal inhibitor of cyclooxygenase-2 (COX-2; also known as Ptgs2a), NS-398, on neutrophil motility in vivo. COX-2 expression is induced at sites of inflammation and produces pro-inflammatory prostaglandins that can be inhibited by NS-398 in animal models, thereby reducing inflammation (Masferrer et al., 1994). NS-398 has been shown to suppress cytokine release (Kimura et al., 2003) and accelerate Fas-mediated apoptosis (Iwase et al., 2006) in human neutrophils,

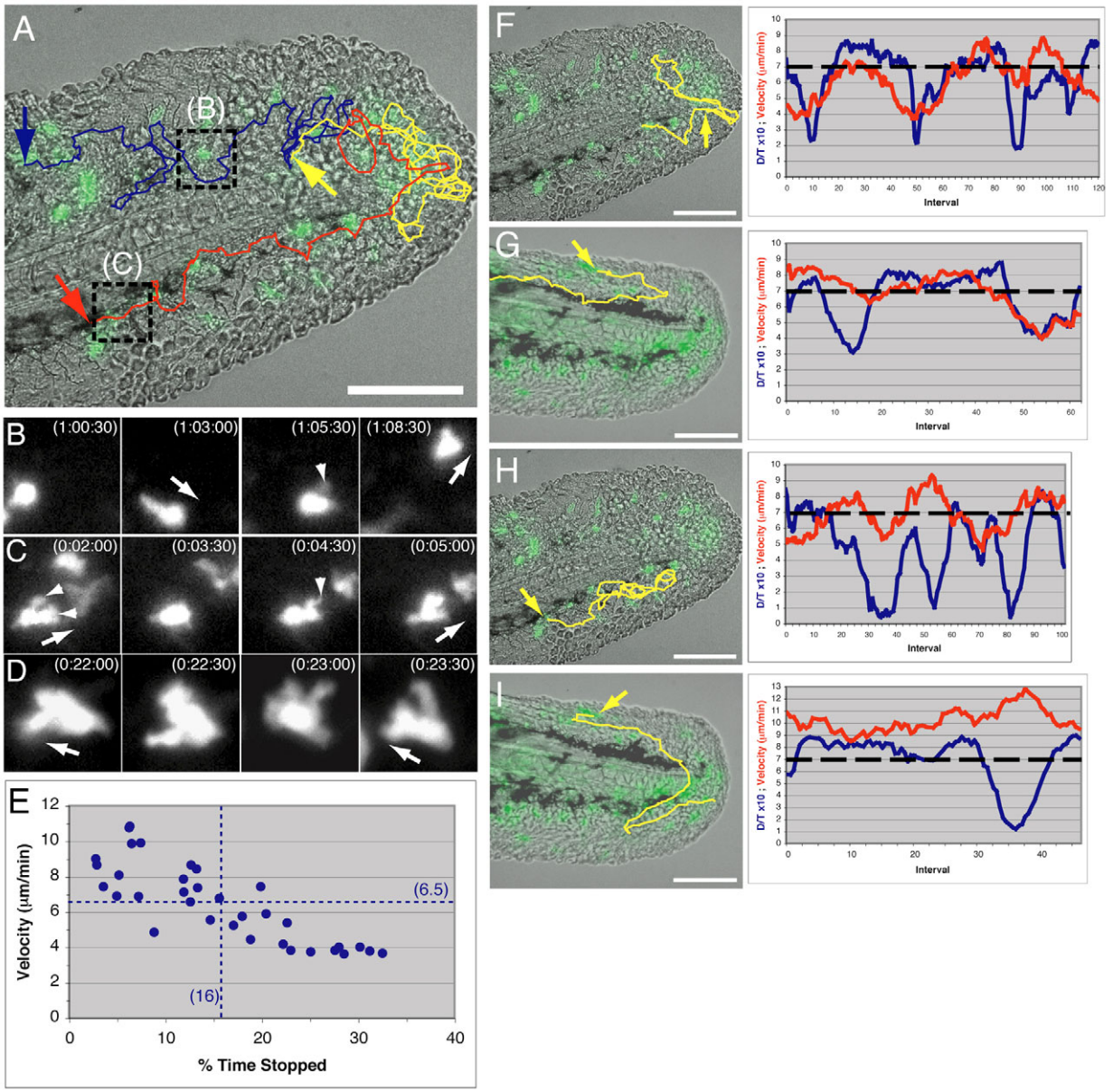

Fig. 7. Migratory behavior of neutrophils in the *hi2217;MPO:GFP* fish. (A) Single frame from time-lapse movie (Movie 1 in supplementary material) of *hi2217;MPO:GFP* embryo tailfin at 2 dpf, fluorescence overlaid onto DIC images. Three individual tracks of GFP-positive neutrophils are shown, with the start of each track indicated with an arrow. Dashed boxes indicate selected segments of tracks, depicted in B and C. Bar, 100 μm. (B,C) Time-lapse sequences of tracks from A, with times indicated at the top of each image in hours:minutes:seconds; the side of each image box equals 50 μm. Large arrows indicate the direction of motility, small arrowheads mark pseudopodia. Note how mutant neutrophils frequently stop and extend pseudopodia. (D) Higher magnification (box side, 25 μm) sequence of a single neutrophil; otherwise same as B,C. Note how several pseudopodia are extended over a 2-minute period. (E) Plot of average velocity against percentage of time stopped (percentage of distance data points less than 0.75 μm) for full-length mutant tracks; each point indicates the parameters for an individual cell, dashed lines indicate the average values (in parentheses) for each data set. (F-I) Analysis of hi2217 mutant neutrophil tracks in 15-minute windows. Single frames from time-lapse movies of *hi2217;MPO:GFP* embryo tailfins at 2 dpf are shown; fluorescence overlaid onto DIC images. Individual tracks of GFP-positive neutrophils are shown, with the start of each track indicated by an arrow; bars, 100 μm. Next to each track image is a plot of directional persistence (D/T, blue lines) and velocity (μm/minute, red lines) over 15-minute time intervals (x axis) for the length of each track. D/T values are multiplied by 10 to use the same numerical y axis as velocity; therefore D/T values above 7 (dashed lines) indicate directional migration.

but to our knowledge its effect on neutrophil migration has not been studied. Mutant embryos incubated in 250 μM NS-398 for 1 hour were observed by time-lapse microscopy in the presence of the drug and after washout. In the presence of NS-398, neutrophil motility was impaired substantially (Fig. 9A,B and Movie 3 in supplementary material). However, migration was rescued after washout of the drug (Fig. 9C and Movie 3 in supplementary material). There was no evidence of

A

	#	V, μm/min	D/T
Mutant	34	6.3 (±3.2)	0.67 (±0.20)
WT Wound	30	8.1 (±2.3)	0.78 (±0.13)
Mutant Wound	27	9.9 (±2.2)	0.77 (±0.13)

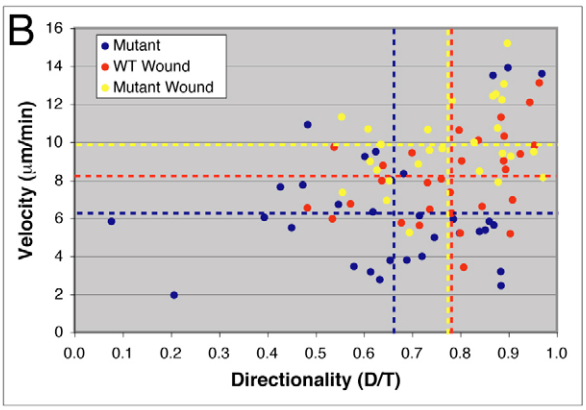

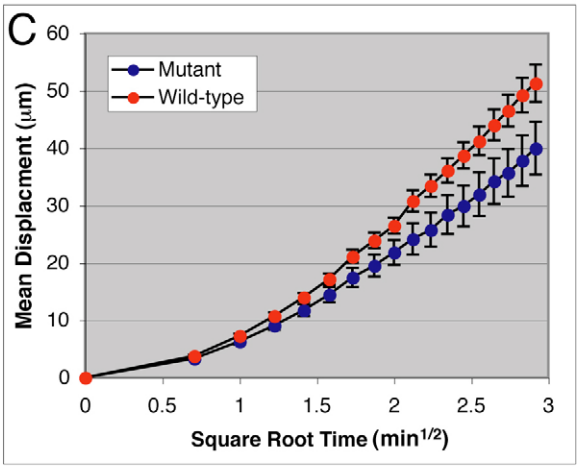

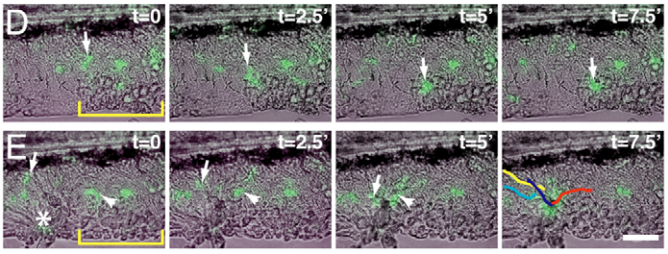

Fig. 8. Neutrophils in *hi2217* mutant embryos display random migration as compared to wild-type neutrophils responding to a wound, but retain the ability to respond directionally to acute injury. (A,B) 'Mutant' data are derived from the first 12 minutes of each *hi2217* mutant track, 'WT Wound' and 'Mutant Wound' data are derived from tracks of neutrophils in response to tailfin wounds in mutants and wild-type siblings, respectively. (A) Table summarizing cell tracking data, including the number of cells tracked (#), average velocity (V, μm/minute) and average directional persistence (D/T); standard deviations are listed in parentheses. (B) Plot of average velocity (μm/minute, y axis) against directionality (D/T, x axis). Each point indicates the parameters for an individual cell; blue points are homozygous mutants, red points are wild-type siblings, yellow points are wounded mutants; dashed lines indicate the average values for each data set. (C) Plot of average mean displacement (μm, y axis) against square root of time interval (minute$^{1/2}$, x axis) for the first 8.5 minute of each track; error bars indicate the standard error of the mean. Blue points are homozygous mutants, red points are derived from tracks of neutrophils in response to tailfin wounds in wild-type siblings. (D,E) Mutant neutrophil response to tissue injury. (D) A homozygous mutant *hi2217;MPO:GFP* embryo at 2 dpf was briefly analyzed by time-lapse microscopy: a single neutrophil (arrows indicate the same cell in each frame) is tracked to an area of cell rounding (yellow brackets) in the ventral fin; indicated times are from the start of the movie. (E) The same embryo was then wounded (indicated with *) to the left of the bracketed area, and neutrophils (arrows or arrowheads mark two individual cells in each frame) were observed to migrate to the wound, with several neutrophils at the wound by 7.5 minutes (indicated times are post-wound). Tracks for four individual neutrophils are overlaid in the last frame. Bar, 50 μm.

neutrophil apoptosis, however, we observed some reduction in heart rate during drug treatment that resolved after washout (data not shown). These findings indicate that the *hi2217;MPO:GFP* zebrafish will be an important tool to assess the effect of inflammatory modulators on neutrophil function in vivo.

Discussion

Here we have demonstrated that zebrafish is an attractive model system to study chronic inflammation because it is genetically tractable, and the optical clarity of zebrafish embryos enables the visualization of inflammatory responses in real-time. This is, to our knowledge, the first chronic inflammation model identified in a zebrafish genetic screen. We now show that Hai1 is a critical regulator of both inflammatory responses and epithelial morphology and proliferation in zebrafish through the regulation of Matriptase 1 activity. Similar epidermal phenotypes have been reported in other mutant zebrafish (Sonawane et al., 2005; van Eeden et al., 1996) however inflammation has not been described in these mutants. The phenotype of epidermal hyperproliferation and inflammation in *hi2217* mutants resembles the common human skin disease psoriasis, and provides an attractive model system to further characterize the relationship between dermal inflammation and epithelial proliferation. These findings demonstrate the validity and feasibility of using zebrafish to study inflammation at the cellular level, and produce a powerful system for the use of genetic and chemical screens for the further identification of molecules that modify the Hai1-Matriptase 1 pathway specifically or have more general effects on inflammation.

Recent studies in mouse models highlight the importance of a balance between Matriptase 1 and Hai1 activity in the progression of epithelial tumors. Dysregulated Matriptase 1 is associated with carcinogenesis and promotes malignant transformation that can be blocked by overexpression of Hai1 in the epidermis (List et al., 2005), suggesting that inhibition of Matriptase 1 may be an attractive target to treat epithelial cancers that are associated with increased Matriptase 1 activity. The *hai1* transgenic zebrafish represents an attractive model to further study the role of Hai1-Matriptase 1 in epithelial hyperproliferation and the generation of inflammation. Inhibition of Matriptase 1 blocks the *hi2217* mutant phenotype

Journal of Cell Science

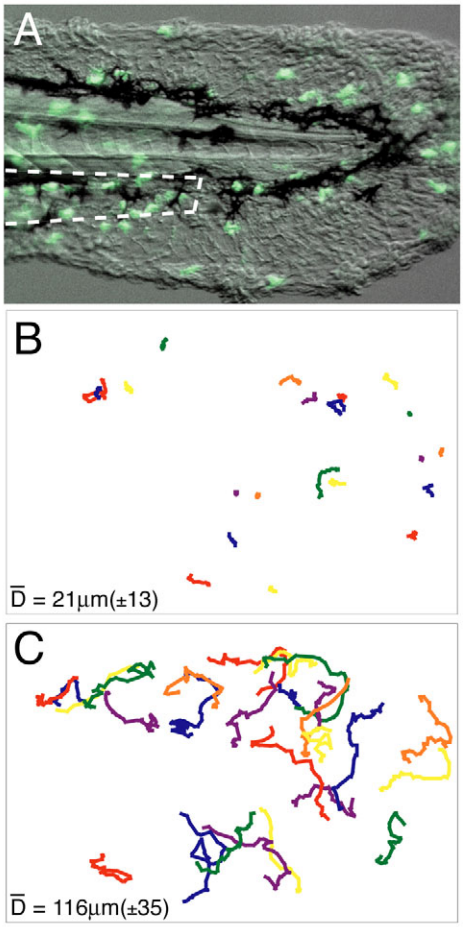

Fig. 9. NS-398 treatment causes neutrophil arrest in *hi2217;MPO:GFP* embryos. (A) Mutant *hi2217;MPO:GFP* embryo tailfin following treatment for 1 hour in 250 μM NS-398. Fluorescence image of the first frame from Movie 3 in supplementary material overlaid onto corresponding OCC image; dashed line indicates the location of the vasculature. (B) Cell tracks of neutrophils from embryo in A, kept in the presence of NS-398. (C) Tracks from same embryo as in A and B, 1 hour after washing out the drug. Average displacements for each set of tracks are indicated in the lower left corner of B and C.

(Fig. 6), providing further support for the utility of this system to understand the relationship between Hai1 and Matriptase 1 in epithelial morphogenesis and inflammation. Furthermore, the transgenic zebrafish model provides a powerful tool to screen for agents that block both the epithelial and inflammatory phenotypes, thereby having therapeutic potential for both inflammatory disease and cancer. The relevance of the zebrafish model to disease models in mice and humans further provides support for the utility of zebrafish genetic screens to identify pathways that regulate the development of chronic inflammation.

The common human skin condition psoriasis is characterized by epithelial proliferation, lack of differentiation and inflammation of the skin (Bowcock and Krueger, 2005; Lowes et al., 2007). The inflammatory infiltrate in psoriasis is often mixed and frequently contains neutrophils. Other inflammatory skin diseases are characterized by a predominantly neutrophilic infiltrate include Sweet syndrome (Wallach and Vignon-Pennamen, 2006) and the autoinflammatory disease neonatal onset multisystem inflammatory disease (NOMID) (Huttenlocher et al., 1995). The phenotype of the *hai1* mutant zebrafish resembles psoriatic disease in that the mutant fish display hyperproliferation of epithelial cells and chronic inflammation. There is a long-standing controversy about whether psoriasis is a primary disease of the keratinocytes or the immune system. Substantial evidence suggests that psoriasis can be a primary disease of keratinocytes, in that changes in gene expression in keratinocytes specifically induces psoriatic disease in mouse models. For example, ectopic expression of beta 1 integrin in mouse keratinocytes induces a disease characterized by keratinocyte hyperproliferation and inflammation with both T cells and neutrophils (Carroll et al., 1995). Our findings further support the importance of primary changes in epithelial function in the pathogenesis of inflammation in the zebrafish fin, as depletion of both neutrophils and macrophages in zebrafish embryos did not block the early morphological phenotypes in *hi2217* mutants (Fig. 4 and supplementary material Fig. S1G′). Further support for a role of the epithelium in orchestrating the inflammatory response in the skin is provided by the production of inducible nitric oxide and IL-8 by epithelial cells in psoriatic lesions (Bruch-Gerharz et al., 1996) that would provide the inflammatory milieu required for the recruitment of neutrophils and other inflammatory cells. Taken together, these findings support the utility of zebrafish inflammation models as systems to study the pathogenesis of epithelial proliferative disorders and their relationship to inflammation. Further studies may help to elucidate the relationship between epithelial phenotypes and inflammation and the development of targets that help to mitigate disease progression.

Whereas the activities of immune cells in normal or tumor contexts have been studied (Bajenoff et al., 2006; Mrass et al., 2006), few studies have addressed the dynamic movement of leukocytes in the context of chronic inflammation in vivo. The zebrafish system represents a powerful model to study the movement of leukocytes in real-time in response to both acute and chronic inflammatory stimuli. Our recent study using zebrafish that express GFP in neutrophils (Mathias et al., 2006) identified a unique mechanism of directional neutrophil trafficking betweens sites of tissue injury and the vasculature, and implicated a novel mechanism of retrograde chemotaxis from wound sites back toward the vasculature in the resolution phase of the inflammatory response. Furthermore, in the context of acute injury we also observed the simultaneous directed migration of individual neutrophils both toward and away from wound sites, suggesting that neutrophils independently respond to signals in an inflammatory context. Using the *hi2217;MPO:GFP* mutant zebrafish, we now demonstrate that in the context of chronic inflammation, zebrafish neutrophils displayed a relatively more random migration within the zebrafish fin, an apparent ‘random walk’ (Fig. 8C) without clear movement toward or away from the vasculature. Analysis of *hai1* mutant cell tracking data indicated that whereas some neutrophils moved in a random manner others demonstrated the ability to move in a directional manner for short periods (Fig. 7A,F-I, Fig. 8B) indicating that

Journal of Cell Science

neutrophils can probably still process and respond to directional signals within an area of chronic inflammation. Accordingly, neutrophils retained the ability to respond to a wound in the mutant embryos. Taken together with our previous observation of directed retrograde migration, the findings suggest that neutrophils in the mutant embryos may still be able to respond to signals that would draw them away from the chronically inflamed area, which presents potential therapeutic applications.

The *hai1* mutant zebrafish embryos displayed diffuse inflammation within the fin by 2 dpf, without aggregates of neutrophils or apparent organization to the inflammatory response. This feature enabled long-term cell tracking of individual neutrophils, with many tracks several hours in length, and created a great advantage for further analysis of cell tracking parameters in vivo (Fig. 7E-I). Although the neutrophils were highly dynamic they frequently exhibited periods of stopping within the zebrafish fin and then subsequent periods of motility (Fig. 7A-C), similar to what has been observed for migrating primordial germ cells (Reichman-Fried et al., 2004). This stopping and starting appeared to be neutrophil-specific and not secondary to localized changes within the extracellular environment, as neutrophils did not aggregate within a specific region of the mutant fin. Upon pausing, neutrophils take on an unpolarized, rounded morphology (Fig. 7B,C) similar to what we have observed when neutrophils stop at a site of tissue injury (Mathias et al., 2006), suggesting that cells within *hi2217* mutant tailfins are producing similar signals that cause neutrophils to arrest. During pauses neutrophils were often observed to extend pseudopodia in multiple directions and then resume migration (Fig. 7B,C), indicating that they are processing multiple directional cues while stopped. Interestingly, treatment with the non-steroidal COX-2 inhibitor NS-398 also induced neutrophils to pause and take on this rounded morphology (Fig. 9A and Movie 3 in supplementary material). Since COX-2 is involved in the production of pro-inflammatory prostaglandins at sites of inflammation, our findings suggest that these inflammatory mediators regulate neutrophil recruitment and migration in vivo. The exact nature of the immune components that trigger the rapid and random motility of neutrophils within the context of this chronic inflammation model remain unknown, however, it likely involves a complex interplay between soluble and extracellular matrix components that impact the inflammatory response. This will be a challenge for future investigations to dissect the molecular architecture of the chronic inflammatory milieu in vivo.

Materials and Methods

Zebrafish maintenance

All protocols using zebrafish in this study were approved by the University of Wisconsin-Madison Research Animal Resources Center. Adult AB zebrafish and embryos were maintained according to standard protocols (Nusslein-Volhard and Dahm, 2002) and staged as previously established (Kimmel et al., 1995). Wounding and endogenous detection of myeloperoxidase activity were performed as described previously (Mathias et al., 2006). Heterozygous *hi2217* adults (official designation *spint1l*^{hi2217}/*spint1l*$^{+}$) were crossed to *Tg(MPO:GFP)*^{uw} (Mathias et al., 2006) transgenic adults and raised; embryos from these adults are referred to in the manuscript as *hi2217;MPO:GFP*.

Image acquisition

Images were captured with either (1) a Nikon SMZ-1500 zoom microscope equipped with epifluorescent illumination (GFP: Ex 470/40, BA 525/50; DsRed: Ex 545/30, BA 525/50), a CoolSnap ES camera (Roper Scientific), and a Digital Sight DS-Fi1 color camera (Nikon); or (2) a Nikon Eclipse TE300 inverted microscope equipped with 20× (NA 0.45), 40× (NA 0.75) and 60× (NA 1.40) DIC objectives, epifluorescent illumination (Ex 480/25, Em 525/40) and a Hamamatsu Orca II CCD camera. For movies, embryos were embedded in 1% low-melting point agarose and maintained in E3 medium containing 0.1 mg/ml Tricaine at 30°C, unless otherwise noted. Color images were captured with NIS Elements D 2.30 software, all other images were captured and analyzed with MetaMorph software. Movies were converted to AVI format using MetaMorph and compressed using QuickTime Player version 7.0.4.

Whole-mount in situ hybridization

The Hopkins mutant zebrafish collection (Amsterdam et al., 1999) was screened for expression of zMPO by in situ hybridization (J.R., unpublished data). Briefly, embryos were obtained from crosses of adults known to be heterozygous for individual insertions, raised in E3 medium containing 0.2 mM *N*-phenylthiourea and fixed at 2 dpf in 4% paraformaldehyde in PBS; zMPO mRNA was labeled by in situ hybridization as described previously (Bennett et al., 2001). Zebrafish *hai1* mRNA expression was detected by the same protocol using probe cb376 (accession # BU492960) as done previously (Thisse et al., 2001). Zebrafish Matriptase 1 was detected using IMAGE clone # 5618275 (obtained from ATCC), a partial cDNA in pBluescript SK– that was digested with either *Xho*I or *Eco*RI to generate templates for sense and antisense probes, respectively.

Zebrafish embryo sectioning

Embryos were fixed as above, washed in PBS, suffused in 30% sucrose and infiltrated with paraffin. Paraffin sections, 5 μm thick, were processed and stained with Hematoxylin and Eosin as described previously (Hsu et al., 2004). Whole-mount in situ-labeled embryos were fixed and suffused in sucrose as above, embedded in OCT and cryosectioned at 10 μm.

Whole-mount immunolabeling, TUNEL and BrdU labeling

Zebrafish embryos were fixed in 4% paraformaldehyde in PBS overnight at 4°C and immunolabeled as described previously (Mathias et al., 2006). Polyclonal antibodies to zebrafish L-plastin as were raised in rabbits following injection of a GST-L-plastin fusion protein (the plasmid construct was a gift from Paul Martin, University of Bristol, UK) and purified as described previously (Bennin et al., 2002). Cadherins were labeled using a polyclonal rabbit anti-Pan-Cadherin IgG (Sigma), which has previously been done in zebrafish (Bitzur et al., 1994; Crawford et al., 2003). Apoptotic cells were fluorescently labeled by terminal deoxynucleotidyl transferase dUTP nick-end labeling (TUNEL) using a Roche kit (catalog # 12156792910) as follows: after immunolabeling, embryos were washed in PBS, placed on ice in 50 μl 1× reaction mix for 1 hour, incubated at 37°C for 1 hour with periodic mixing and washed as in the immunolabeling protocol. Proliferating cells were labeled by incubating embryos in 10 mM 5-bromo-deoxyuridine (BrdU) in E3 for 20 minutes (Dekens et al., 2003b); embryos were then washed in E3, fixed and processed as described for immunolabeling, except that following rehydration from methanol embryos were treated with 4 M HCl for 20 minutes (Dekens et al., 2003a) and washed in PBS several times. BrdU-labeled cells were detected with a monoclonal antibody to BrdU (Sigma, clone BU33) and a Rhodamine Red-conjugated goat anti-mouse antibody (Molecular Probes).

Morpholino oligonucleotide microinjection

Morpholino oligonucleotides (MO) were purchased from GeneTools, LLC (Philomath, OR, USA) and resuspended 1× Danieau buffer to a stock concentration of 1 mM, according to the manufacturer's protocols. MO were further diluted in 1× Danieau buffer and injected (amounts indicated below with each individual MO) into the yolk of 1- to 4-cell stage embryos; control MO were injected at the same (or greater) volume and concentration. Standard control MO sequence is available from GeneTools, pu.1 (1 nl at 1 mM injected) and p53 (1 nl at 1 mM) MO sequences were as described previously (Langheinrich et al., 2002; Rhodes et al., 2005). Other MO sequences were designed to block translation (*hai1*: accession no. BC053239; *matriptase 1*: accession no. XM_678577) and are as follows (5′-3′):
hai1 (0.5 nl at 35 μM) – CTGAGTTGAGCCAGAGTCATCCTCC
hai1, 5-base mismatch – CTcAGTTcAGCCAcAGTgATgCTCC
matriptase 1 MO1 (0.2-0.5 nl at 0.3 mM) – GCATTCCTCCATCCATAGGGTCCAT
matriptase 1 MO1, 5-base mismatch – GCATTgCTCgATgCATAcGGTCgAT
matriptase 1 MO2 (0.4-0.5 nl at 0.3 mM) – CCACTGGCAGAATCAAAATCA-ACAC.

For injection into 8- to 16-cell embryos (Fig. 5D,E), either the *hai1* or 5-base mismatch *hai1* MO was diluted to 0.65 μM in 1× Danieau along with 5 mg/ml tetramethyl Rhodamine-conjugated dextran (MW=10,000; Molecular Probes) as a cell tracer; 66 pl was then injected into single cells. For partial knock-down of *matriptase 1* (Fig. 6K,L), 0.25 nl of 0.3 mM *matriptase 1* MO2 were injected into the yolk of *hi2217* embryos.

Cell tracking and analysis

Neutrophils from *hi2217;MPO:GFP* embryos were tracked and analyzed as described previously (Mathias et al., 2006); data were collected from three movies

for both mutant embryos and wild-type siblings with wounded tailfins. For Fig. 7, tracks in mutants include all data points in which an individual cell can be distinguished from other cells. To derive percentage time stopped (Fig. 7E), values for each overall mutant cell track, the number of data points in which the distance traveled was less than 0.75 μm was divided by the total data time points. For the analysis in Fig. 7F-I velocity and D/T values were determined for successive 15-minute intervals of the track with 1 minute between each interval, i.e. parameters for interval 1 were derived from coordinates at time points t_1=1 minute and t_2=15 minutes, interval 2 from t_1=2 minutes and t_2=16 minutes, and so on until the end of the track. For comparison of wild-type cell tracks to the significantly longer overall mutant cell tracks, the average length of wild-type cell tracks to wounds was determined to be 12 minutes; therefore the first 12 minutes of each mutant cell track (starting at the onset of migration) was taken and parameters were derived for Fig. 8A,B. For Fig. 8C, the first 8.5 minutes of individual tracks (starting at the onset of migration, omitting pauses that start some tracks) were used to calculate mean displacement values (Sumen et al., 2004).

NS-398 drug treatment

Mutant embryos were washed in E3 containing 0.1% DMSO and 0.2% BSA (E3++), then incubated for 1 hour at room temperature in E3++ supplemented with either 250 μM NS-398 (purchased either from Sigma or Cayman Chemical and resuspended at 5 mg/ml in DMSO) or 1.5% DMSO (as a vehicle control). Tricaine was then added to a final concentration of 0.1 mg/ml and movies were captured as detailed above, except that embryos were not embedded in agarose. Imaged embryos were then washed several times in E3++ and allowed to recover for 1 hour, followed by further imaging of the same embryos.

We gratefully acknowledge Adam Amsterdam, Sarah Farrington and Nancy Hopkins (M.I.T.) for providing *hi2217* zebrafish embryos, Satoshi Kinoshita for embryo sectioning and staining, David Bennin for production of L-Plastin antibodies, and Brian Kayon for maintenance of the zebrafish facility and other work supporting this study. This work was supported by NIH grants to A.H. (R01 GM074827), J.R. (5KO1DK69672), C. B. Thisse (RR15402-01, for provision of cb376 EST) and the Department of Medicine at the University of Wisconsin-Madison (M.E.D.), and an Arthritis Foundation post-doctoral fellowship (J.R.M.). The authors declare no conflicts of interest related to this work.

References

Amsterdam, A., Burgess, S., Golling, G., Chen, W., Sun, Z., Townsend, K., Farrington, S., Haldi, M. and Hopkins, N. (1999). A large-scale insertional mutagenesis screen in zebrafish. *Genes Dev.* **13**, 2713-2724.

Amsterdam, A., Nissen, R. M., Sun, Z., Swindell, E. C., Farrington, S. and Hopkins, N. (2004). Identification of 315 genes essential for early zebrafish development. *Proc. Natl. Acad. Sci. USA* **101**, 12792-12797.

Bajenoff, M., Egen, J. G., Koo, L. Y., Laugier, J. P., Brau, F., Glaichenhaus, N. and Germain, R. N. (2006). Stromal cell networks regulate lymphocyte entry, migration, and territoriality in lymph nodes. *Immunity* **25**, 989-1001.

Benaud, C., Dickson, R. B. and Lin, C. Y. (2001). Regulation of the activity of matriptase on epithelial cell surfaces by a blood-derived factor. *Eur. J. Biochem.* **268**, 1439-1447.

Bennett, C. M., Kanki, J. P., Rhodes, J., Liu, T. X., Paw, B. H., Kieran, M. W., Langenau, D. M., Delahaye-Brown, A., Zon, L. I., Fleming, M. D. et al. (2001). Myelopoiesis in the zebrafish, Danio rerio. *Blood* **98**, 643-651.

Bennin, D. A., Don, A. S., Brake, T., McKenzie, J. L., Rosenbaum, H., Ortiz, L., DePaoli-Roach, A. A. and Horne, M. C. (2002). Cyclin G2 associates with protein phosphatase 2A catalytic and regulatory B' subunits in active complexes and induces nuclear aberrations and a G1/S phase cell cycle arrest. *J. Biol. Chem.* **277**, 27449-27467.

Bitzur, S., Kam, Z. and Geiger, B. (1994). Structure and distribution of N-cadherin in developing zebrafish embryos: morphogenetic effects of ectopic over-expression. *Dev. Dyn.* **201**, 121-136.

Bowcock, A. M. and Krueger, J. G. (2005). Getting under the skin: the immunogenetics of psoriasis. *Nat. Rev. Immunol.* **5**, 699-711.

Bruch-Gerharz, D., Fehsel, K., Suschek, C., Michel, G., Ruzicka, T. and Kolb-Bachofen, V. (1996). A proinflammatory activity of interleukin 8 in human skin: expression of the inducible nitric oxide synthase in psoriatic lesions and cultured keratinocytes. *J. Exp. Med.* **184**, 2007-2012.

Carroll, J. M., Romero, M. R. and Watt, F. M. (1995). Suprabasal integrin expression in the epidermis of transgenic mice results in developmental defects and a phenotype resembling psoriasis. *Cell* **83**, 957-968.

Crawford, B. D., Henry, C. A., Clason, T. A., Becker, A. L. and Hille, M. B. (2003). Activity and distribution of paxillin, focal adhesion kinase, and cadherin indicate cooperative roles during zebrafish morphogenesis. *Mol. Biol. Cell* **14**, 3065-3081.

Crowhurst, M. O., Layton, J. E. and Lieschke, G. J. (2002). Developmental biology of zebrafish myeloid cells. *Int. J. Dev. Biol.* **46**, 483-492.

Davis, J. M., Clay, H., Lewis, J. L., Ghori, N., Herbomel, P. and Ramakrishnan, L. (2002). Real-time visualization of mycobacterium-macrophage interactions leading to initiation of granuloma formation in zebrafish embryos. *Immunity* **17**, 693-702.

de Jong, J. L. and Zon, L. I. (2005). Use of the zebrafish system to study primitive and definitive hematopoiesis. *Annu. Rev. Genet.* **39**, 481-501.

Dekens, M. P., Pelegri, F. J., Maischein, H. M. and Nusslein-Volhard, C. (2003a). The maternal-effect gene futile cycle is essential for pronuclear congression and mitotic spindle assembly in the zebrafish zygote. *Development* **130**, 3907-3916.

Dekens, M. P., Santoriello, C., Vallone, D., Grassi, G., Whitmore, D. and Foulkes, N. S. (2003b). Light regulates the cell cycle in zebrafish. *Curr. Biol.* **13**, 2051-2057.

Fan, B., Brennan, J., Grant, D., Peale, F., Rangell, L. and Kirchhofer, D. (2006). Hepatocyte growth factor activator inhibitor-1 (HAI-1) is essential for the integrity of basement membranes in the developing placental labyrinth. *Dev. Biol.* **303**, 222-230.

Hall, C., Flores, M. V., Storm, T., Crosier, K. and Crosier, P. (2007). The zebrafish lysozyme C promoter drives myeloid-specific expression in transgenic fish. *BMC Dev. Biol.* **7**, 42.

Hsu, K., Traver, D., Kutok, J. L., Hagen, A., Liu, T. X., Paw, B. H., Rhodes, J., Berman, J. N., Zon, L. I., Kanki, J. P. et al. (2004). The pu.1 promoter drives myeloid gene expression in zebrafish. *Blood* **104**, 1291-1297.

Huttenlocher, A., Frieden, I. J. and Emery, H. (1995). Neonatal onset multisystem inflammatory disease. *J. Rheumatol.* **22**, 1171-1173.

Iwase, M., Takaoka, S., Uchida, M., Kondo, G., Watanabe, H., Ohashi, M. and Nagumo, M. (2006). Accelerative effect of a selective cyclooxygenase-2 inhibitor on Fas-mediated apoptosis in human neutrophils. *Int. Immunopharmacol.* **6**, 334-341.

Kimmel, C. B., Ballard, W. W., Kimmel, S. R., Ullmann, B. and Schilling, T. F. (1995). Stages of embryonic development of the zebrafish. *Dev. Dyn.* **203**, 253-310.

Kimura, T., Iwase, M., Kondo, G., Watanabe, H., Ohashi, M., Ito, D. and Nagumo, M. (2003). Suppressive effect of selective cyclooxygenase-2 inhibitor on cytokine release in human neutrophils. *Int. Immunopharmacol.* **3**, 1519-1528.

Langenau, D. M. and Zon, L. I. (2005). The zebrafish: a new model of T-cell and thymic development. *Nat. Rev. Immunol.* **5**, 307-317.

Langenau, D. M., Ferrando, A. A., Traver, D., Kutok, J. L., Hezel, J. P., Kanki, J. P., Zon, L. I., Look, A. T. and Trede, N. S. (2004). In vivo tracking of T cell development, ablation, and engraftment in transgenic zebrafish. *Proc. Natl. Acad. Sci. USA* **101**, 7369-7374.

Langheinrich, U., Hennen, E., Stott, G. and Vacun, G. (2002). Zebrafish as a model organism for the identification and characterization of drugs and genes affecting p53 signaling. *Curr. Biol.* **12**, 2023-2028.

Lee, S. L., Dickson, R. B. and Lin, C. Y. (2000). Activation of hepatocyte growth factor and urokinase/plasminogen activator by matriptase, an epithelial membrane serine protease. *J. Biol. Chem.* **275**, 36720-36725.

Lieschke, G. J., Oates, A. C., Crowhurst, M. O., Ward, A. C. and Layton, J. E. (2001). Morphologic and functional characterization of granulocytes and macrophages in embryonic and adult zebrafish. *Blood* **98**, 3087-3096.

List, K., Szabo, R., Molinolo, A., Sriuranpong, V., Redeye, V., Murdock, T., Burke, B., Nielsen, B. S., Gutkind, J. S. and Bugge, T. H. (2005). Deregulated matriptase causes ras-independent multistage carcinogenesis and promotes ras-mediated malignant transformation. *Genes Dev.* **19**, 1934-1950.

Lowes, M. A., Bowcock, A. M. and Krueger, J. G. (2007). Pathogenesis and therapy of psoriasis. *Nature* **445**, 866-873.

Masferrer, J. L., Zweifel, B. S., Manning, P. T., Hauser, S. D., Leahy, K. M., Smith, W. G., Isakson, P. C. and Seibert, K. (1994). Selective inhibition of inducible cyclooxygenase 2 in vivo is antiinflammatory and nonulcerogenic. *Proc. Natl. Acad. Sci. USA* **91**, 3228-3232.

Mathias, J. R., Perrin, B. J., Liu, T. X., Kanki, J., Look, A. T. and Huttenlocher, A. (2006). Resolution of inflammation by retrograde chemotaxis of neutrophils in transgenic zebrafish. *J. Leukoc. Biol.* **80**, 1281-1288.

Meijer, A. H., van der Sar, A. M., Cunha, C., Lamers, G. E., Laplante, M. A., Kikuta, H., Bitter, W., Becker, T. S. and Spaink, H. P. (2007). Identification and real-time imaging of a myc-expressing neutrophil population involved in inflammation and mycobacterial granuloma formation in zebrafish. *Dev. Comp. Immunol.* May 22 [Epub ahead of print] doi:10.1016/j.dci.2007.04.003

Miyazawa, K., Shimomura, T., Naka, D. and Kitamura, N. (1994). Proteolytic activation of hepatocyte growth factor in response to tissue injury. *J. Biol. Chem.* **269**, 8966-8970.

Mrass, P., Takano, H., Ng, L. G., Daxini, S., Lasaro, M. O., Iparraguirre, A., Cavanagh, L. L., von Andrian, U. H., Ertl, H. C., Haydon, P. G. et al. (2006). Random migration precedes stable target cell interactions of tumor-infiltrating T cells. *J. Exp. Med.* **203**, 2749-2761.

Murayama, E., Kissa, K., Zapata, A., Mordelet, E., Briolat, V., Lin, H. F., Handin, R. I. and Herbomel, P. (2006). Tracing hematopoietic precursor migration to successive hematopoietic organs during zebrafish development. *Immunity* **25**, 963-975.

Nusslein-Volhard, C. and Dahm, R. (2002). *Zebrafish, A Practical Approach*. New York: Oxford University Press.

Oberst, M., Anders, J., Xie, B., Singh, B., Ossandon, M., Johnson, M., Dickson, R. B. and Lin, C. Y. (2001). Matriptase and HAI-1 are expressed by normal and malignant epithelial cells in vitro and in vivo. *Am. J. Pathol.* **158**, 1301-1311.

Onnebo, S. M., Yoong, S. H. and Ward, A. C. (2004). Harnessing zebrafish for the study of white blood cell development and its perturbation. *Exp. Hematol.* **32**, 789-796.

Patton, E. E. and Zon, L. I. (2001). The art and design of genetic screens: zebrafish. *Nat. Rev. Genet.* **2**, 956-966.

Redd, M. J., Kelly, G., Dunn, G., Way, M. and Martin, P. (2006). Imaging macrophage chemotaxis in vivo: studies of microtubule function in zebrafish wound inflammation. *Cell Motil. Cytoskeleton* **63**, 415-422.

Journal of Cell Science

Reichman-Fried, M., Minina, S. and Raz, E. (2004). Autonomous modes of behavior in primordial germ cell migration. *Dev. Cell* **6**, 589-596.

Renshaw, S. A., Loynes, C. A., Trushell, D. M., Elworthy, S., Ingham, P. W. and Whyte, M. K. (2006). A transgenic zebrafish model of neutrophilic inflammation. *Blood* **108**, 3976-3978.

Rhodes, J., Hagen, A., Hsu, K., Deng, M., Liu, T. X., Look, A. T. and Kanki, J. P. (2005). Interplay of pu.1 and gata1 determines myelo-erythroid progenitor cell fate in zebrafish. *Dev. Cell* **8**, 97-108.

Santin, A. D., Cane, S., Bellone, S., Bignotti, E., Palmieri, M., De Las Casas, L. E., Anfossi, S., Roman, J. J., O'Brien, T. and Pecorelli, S. (2003). The novel serine protease tumor-associated differentially expressed gene-15 (matriptase/MT-SP1) is highly overexpressed in cervical carcinoma. *Cancer* **98**, 1898-1904.

Shi, Y. E., Torri, J., Yieh, L., Wellstein, A., Lippman, M. E. and Dickson, R. B. (1993). Identification and characterization of a novel matrix-degrading protease from hormone-dependent human breast cancer cells. *Cancer Res.* **53**, 1409-1415.

Shimomura, T., Denda, K., Kitamura, A., Kawaguchi, T., Kito, M., Kondo, J., Kagaya, S., Qin, L., Takata, H., Miyazawa, K. et al. (1997). Hepatocyte growth factor activator inhibitor, a novel Kunitz-type serine protease inhibitor. *J. Biol. Chem.* **272**, 6370-6376.

Sonawane, M., Carpio, Y., Geisler, R., Schwarz, H., Maischein, H. M. and Nuesslein-Volhard, C. (2005). Zebrafish penner/lethal giant larvae 2 functions in hemidesmosome formation, maintenance of cellular morphology and growth regulation in the developing basal epidermis. *Development* **132**, 3255-3265.

Sumen, C., Mempel, T. R., Mazo, I. B. and von Andrian, U. H. (2004). Intravital microscopy: visualizing immunity in context. *Immunity* **21**, 315-329.

Tanaka, H., Nagaike, K., Takeda, N., Itoh, H., Kohama, K., Fukushima, T., Miyata, S., Uchiyama, S., Uchinokura, S., Shimomura, T. et al. (2005). Hepatocyte growth factor activator inhibitor type 1 (HAI-1) is required for branching morphogenesis in the chorioallantoic placenta. *Mol. Cell. Biol.* **25**, 5687-5698.

Thisse, B., Pflumio, S., Fürthauer, M., Loppin, B., Heyer, V., Degrave, A., Woehl, R., Lux, A., Steffan, T., Charbonnier, X. et al. (2001). Expression of the zebrafish genome during embryogenesis (spint1l/HAI-1). *ZFIN Direct Data Submission*, http://zfin.org/cgi-bin/webdriver?MIval=aa-fxallfigures.apg&OID=ZDB-PUB-010810-1&fxallfig_probe_zdb_id=ZDB-EST-020912-19.

Trede, N. S., Langenau, D. M., Traver, D., Look, A. T. and Zon, L. I. (2004). The use of zebrafish to understand immunity. *Immunity* **20**, 367-379.

van der Sar, A. M., Musters, R. J., van Eeden, F. J., Appelmelk, B. J., Vandenbroucke-Grauls, C. M. and Bitter, W. (2003). Zebrafish embryos as a model host for the real time analysis of Salmonella typhimurium infections. *Cell. Microbiol.* **5**, 601-611.

van Eeden, F. J., Granato, M., Schach, U., Brand, M., Furutani-Seiki, M., Haffter, P., Hammerschmidt, M., Heisenberg, C. P., Jiang, Y. J., Kane, D. A. et al. (1996). Genetic analysis of fin formation in the zebrafish, *Danio rerio*. *Development* **123**, 255-262.

Wallach, D. and Vignon-Pennamen, M. D. (2006). From acute febrile neutrophilic dermatosis to neutrophilic disease: forty years of clinical research. *J. Am. Acad. Dermatol.* **55**, 1066-1071.

Zon, L. I. and Peterson, R. T. (2005). In vivo drug discovery in the zebrafish. *Nat. Rev. Drug Discov.* **4**, 35-44.

Journal of Cell Science